Journal of Zhejiang University-SCIENCE C (Computers & Electronics)
ISSN 1869-1951 (Print); ISSN 1869-196X (Online)
www.zju.edu.cn/jzus; www.springerlink.com
E-mail: jzus@zju.edu.cn

Feedback analysis and design of inductive power links driven by Class-E amplifiers with variable coupling coefficients*

Tian-liang YANG†, Chun-yu ZHAO, Da-yue CHEN†‡

(*Institute of Intelligent Mechatronics Research, School of Electronic, Information and Electrical Engineering, Shanghai Jiao Tong University, Shanghai 200240, China*)

†E-mail: {tlyang, dychen}@sjtu.edu.cn

Received Oct. 12, 2009; Revision accepted May 10, 2010; Crosschecked July 16, 2010

Abstract: The efficiency of inductive power links driven by Class-E amplifiers may deteriorate due to variation in the coupling coefficient when the relative position of the radio frequency (RF) coils changes. To solve this problem, a new design methodology of power links is presented in this paper. The aim of the new design is to use the feedback signal, which is a phase difference between the driving signal and the output current of the Class-E amplifier, to adjust the duty cycle and angular frequency of the driving signal to maintain the optimum state of the inductive power link, and to adjust the supply voltage to keep the output power constant when the coupling coefficient of the RF coils changes. The parameter adjustments with respect to the coupling coefficient and the feedback signal are derived from the design equation of the inductive power link. To validate the feedback control rules, a prototype of the inductive power link was constructed, and its performance validated with the coupling coefficient set at 0.2 and a duty cycle of 0.5. The experimental results showed that, by adjusting the duty cycle, the angular frequency, and the supply voltage, the power link can be kept in optimal operation with a constant output power when the coupling coefficient changes from 0.2 to 0.1 to 0.25.

Key words: Inductive power link, Closed-loop Class-E amplifier, High efficient, Variable coupling coefficient
doi:10.1631/jzus.C0910607 **Document code:** A **CLC number:** TN721.2

1 Introduction

Inductive power links driven by Class-E amplifiers are commonly used to power implantable biomedical devices (Sarpeshkar *et al.*, 2005; Lenaerts and Puers, 2007). An increasing trend is to use rechargeable implanted batteries to power such devices, which require periodical recharging through a power link. A basic structure of the inductive power links is shown in Fig. 1 (Baker and Rahul, 2007).

The Class-E amplifier drives the primary radio frequency (RF) coil. The coil then sends inductive power to the secondary RF coil through the skin of the patient. A power supply can be created by rectifying the RF signal on the secondary coil, which can then be used to charge the implanted battery. The center distance between the RF coil pair is d. Variation in d and displacement of the RF coil pair can affect the coupling coefficient k, and hence change the operating state of the power link.

The inductive power link is expected to be of high efficiency to prolong the feeding duration of the battery and reduce the possibility of tissue damage caused by overheating. It is also expected to have constant output power or constant output voltage so that the implanted devices can work in the normal state. However, because of body movements, displacement of the inductive coils or variation in the distance between them may occur leading to variation in k. Consequently, the efficiency may decrease and the output power may change. Previous studies reported that when k changes, the Class-E amplifier may be returned to a better or optimum operating state

‡ Corresponding author
* Project (No. 60271031) supported by the National Natural Science Foundation of China

by adjusting the frequency (Kendir *et al*., 2005; Zan *et al.*, 2007). However, the frequency adjustment ranges have not yet been determined theoretically. When the transmitting coil is flexible or deformable, an electrically controllable inductance is employed to compensate for changes in the transmitting coil (Lenaerts and Puers, 2008). However, variation in k will lead to variation in the impedance that the secondary circuit reflects to the primary circuit, and the inductance compensation cannot retune the power link. The output power will vary due to the variation in k. It can be kept constant or be varied as designated by increasing or decreasing the supply voltage of the primary circuit according to the data sent back by the secondary circuit (Wang *et al.*, 2005). However, the efficiency may deteriorate due to the loss of the optimum state.

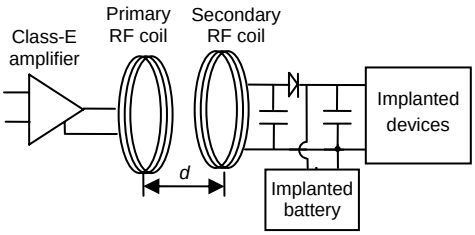

Fig. 1 Example of an inductive power link for implanted devices

In this paper, a design methodology is presented for an inductive power link driven by a Class-E amplifier with the aim of improving efficiency and keeping the output power constant when k changes. Analytical expressions are derived as functions of the duty cycle D and the angular frequency ω_0 of the driving signal. The phase difference θ_{PD} between the output current of the Class-E amplifier and the driving signal is used as a feedback quantity; D, ω_0, and V_{DD} are designated as the adjusted parameters. The relations between the adjusted parameters and k as well as θ_{PD} are obtained from the design equations of the inductive link with k=0.2 and D=0.5. Experiments were conducted to validate the theoretical design when k is changed from 0.2 to 0.1 to 0.25.

2 Determination of component values

To simplify the derivation of the analytical equation parameter of each component, the load resistances of the secondary circuit are equivalent to one resistance R_L. The nonlinear secondary circuit is converted to a linear model by transferring the DC load to an equivalent AC load (Fig. 2) (Ko *et al*., 1977; Donaldson and Perkins, 1983).

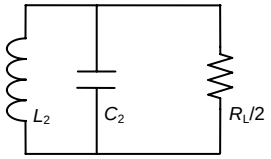

Fig. 2 Approximated linear model of the secondary circuit
L_2 is the secondary RF coil and C_2 is the resonant capacitance

The RF coil pair links the primary and secondary circuits, and the reflected impedance of the secondary circuit appearing at the primary circuit, Z'_{eL}, is defined by

$$\begin{aligned} Z'_{eL} &= \omega_0^2 M^2 / Z_2 \\ &= \frac{\omega_0^2 k^2 L_1 L_2 (4+\omega_0^2 C_2^2 R_L^2)}{4R_L^2 + \left[\omega_0 L_2 (4+\omega_0^2 C_2^2 R_L^2) - \omega_0 C_2 R_L^2\right]^2} \\ &\quad \cdot \left\{2R_L - \mathrm{j}\left[\omega_0 L_2 (4+\omega_0^2 C_2^2 R_L^2) - \omega_0 C_2 R_L^2\right]\right\} \\ &= R'_{eL} + \mathrm{j}X'_{eL}, \end{aligned} \tag{1}$$

where ω_0 is the angular frequency, $M=k\sqrt{L_1 L_2}$ is the mutual inductance between the transmitter coils L_1 and L_2, k is the coupling coefficient, Z_2 is the secondary impedance from the mutual inductance, R'_{eL} is the reflected resistance, and X'_{eL} is the reflected reactance.

The primary circuit is a basic Class-E amplifier. Fig. 3 shows the schematic diagram of the primary circuit with an equivalent impedance Z_{eL}.

To enable the inductive power link to operate in the optimum state, the reflected impedance of the secondary circuit is required to equal the equivalent impedance of the Class-E amplifier; i.e., the design equation of the inductive power link can be expressed by

$$Z'_{eL} = Z_{eL}. \tag{2}$$

Z'_{eL} can be derived from Eq. (1) and Z_{eL} can be obtained from the design equations of the Class-E amplifier. To derive the design equations, the following analysis is performed on the assumptions that

L_f is lossless and large enough to neglect its ripple current, and that the load quality factor Q of the series-resonant circuit is high enough so that the output current can be considered a sine wave.

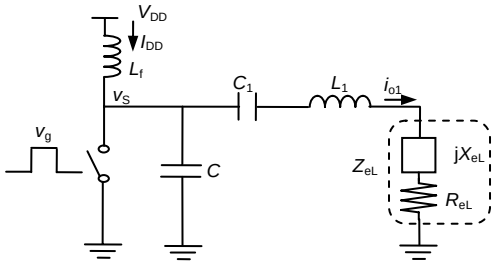

Fig. 3 Schematic diagram of the primary circuit with an equivalent impedance

A basic Class-E amplifier consists of an ideal switch, a shunt capacitance C, an RF choke coil L_f, and a series-resonant circuit comprising L_1, a capacitance C_1, and an equivalent load impedance Z_{eL}. Z_{eL}, which is composed of an equivalent resistance R_{eL} and an equivalent reactance X_{eL}, is defined as an equivalent impedance that lets the Class-E amplifier operate in the optimum state. v_g is the driving signal, which has a duty cycle D and an angular frequency ω_0. v_S is the switch voltage

The output current i_{o1} of the Class-E amplifier can be expressed as

$$i_{o1}(\theta) = I_{o1m} \sin\theta, \tag{3}$$

where I_{o1m} is the current amplitude and $\theta=\omega_0 t$ is the phase.

To satisfy the zero-derivative switching (ZDS) condition (Sokal and Sokal, 1975; Raab, 1977), the switch should turn on at the instant that i_{o1} is equal to the supply current I_{DD}. The relationship between I_{DD} and i_{o1} can be expressed as

$$I_{DD} = I_{o1m} \sin\theta_X, \tag{4}$$

where $\theta_X=\pi-\theta_{PD}$, and θ_{PD} is the phase difference between v_g and i_{o1}. θ_X can be determined by the zero-voltage switching (ZVS) condition (Sokal and Sokal, 1975; Raab, 1977) as

$$\theta_X = \arctan\left(\frac{1-\cos\theta_D}{2\pi-\theta_D+\sin\theta_D}\right), \tag{5}$$

where $\theta_D=2\pi D$ is the switch-on phase duration.

In the switch-off duration, the current of shunt capacitance $i_C=I_{DD}-i_{o1}$, and in the switch-on duration, $i_C=0$. In a switch-off and switch-on cycle, the DC component of i_C is zero because of the ZVS condition. The switch voltage v_S can be expressed as $V_S(j\omega)=I_C(j\omega)/(j\omega C)$ in the frequency domain, where V_S and I_C are the Fourier transforms of v_S and i_C, respectively. The voltage drop of L_f is zero since L_f is lossless. Hence the supply voltage V_{DD} equals the DC component of $V_S(j\omega)$, i.e., $V_{DD}=V_S(0)$. V_{DD} can be expressed as

$$V_{DD} = \frac{I_{o1m}}{2\pi\omega_0 C}\alpha, \tag{6}$$

where $\alpha=-\theta_F\theta_c\sin\theta_X+\theta_F\cos(\theta_D/2)\cos\theta_c+2\sin(\theta_D/2)\times\cos\theta_c+2\theta_c\sin(\theta_D/2)\sin\theta_c$, $\theta_F=2\pi-\theta_D$, and $\theta_c=\theta_D-\theta_X$.

The load impedance of the Class-E amplifier at ω_0 can be expressed as $Z_{1L}=R_{eL}+j[X_{eL}+\omega_0 L_1-1/(\omega_0 C_1)]$. It can also be obtained by $Z_{1L}=V_s(\omega_0)/I_{o1}(\omega_0)$, where $V_s(\omega_0)$ and $I_{o1}(\omega_0)$ are the spectral components of V_S and I_{o1} respectively at ω_0. Comparing the two expressions of Z_{1L}, the real and imaginary parts of Z_{1L} can be obtained by

$$R_{eL} = \beta/(2\pi\omega_0 C) \tag{7}$$

and

$$X_{eL} = \gamma/(2\pi\omega_0 C) - \omega_0 L_1 + 1/(\omega_0 C_1), \tag{8}$$

where $\beta=[\sin\theta_X+\sin(\theta_D-\theta_X)]^2$ and $\gamma=\theta_F\cos(2\theta_X)+\sin\theta_D\cos(2\theta_c)$. α, β, and γ are functions of D. Eqs. (7) and (8) are the design equations of the Class-E amplifier. When the component values satisfy the design equations, the Class-E amplifier will operate in the optimum state.

In the power link, D, V_{DD}, and the output power P_{out} are always designated as the given parameters. P_{out} is equal to both the transmitting power P_{RF} and the input power P_{in} if the parasitic resistance of each component is zero. From Eqs. (4), (6), and (7), R_{eL} can be expressed in terms of P_{in}, V_{DD}, and D as

$$R_{eL} = \frac{\beta\sin\theta_X V_{DD}^2}{\alpha P_{in}}. \tag{9}$$

With the calculated R_{eL}, C can be determined by Eq. (7). L_1 can be obtained by $L_1=QR_{eL}/\omega_0$ with a given Q. L_f is expected to be large enough, but it will take a long time to reach steady state if L_f is too large. L_f can be determined by $L_f=4\pi(\pi^2/4+1)R_{eL}/\omega_0$ (Kazimierczuk

and Czarkowski, 1995).

Combining Eqs. (1), (7), and (8), the resonant capacitance C_2 can be determined by the resonant condition ($\omega_0 = 1/\sqrt{L_2 C_2}$) as

$$C_2 = \frac{2R_{\mathrm{eL}}}{\omega_0^2 k^2 L_1 R_{\mathrm{L}}}. \tag{10}$$

L_2 can then be obtained by the resonant condition. X_{eL} can be obtained from Eq. (1). Finally, C_1 is determined by Eq. (8).

In previous studies, X_{eL} was always designated as 0 to facilitate the component determination of the Class-E amplifier, and the operating frequency was slightly smaller than the resonant frequency of L_2 and C_2 (Donaldson and Perkins, 1983). In our design, X_{eL} is a capacity reactance. From Eq. (1), X_{eL} is derived by

$$X_{\mathrm{eL}} = -k^2 \omega_0 L_1. \tag{11}$$

The power link with the calculated component values will meet the design Eq. (2) and then will operate in the optimum state when k is equal to the designated values.

3 Feedback analysis

3.1 Variation in the coupling coefficient

When k varies, the power link will deviate from its optimum state. The efficiency will deteriorate and the output power will change. Adjustments are required to improve the efficiency and keep the output power constant. In the following analysis, D and ω_0 are employed as adjustments for re-tuning the power link, and the adjustment of V_{DD} is used to keep P_{out} constant. By using the experimental parameters shown later in Table 2, D, ω_0, and V_{DD} with respect to k are obtained from the design Eq. (2).

Substituting Eqs. (1), (7), and (8) into Eq. (2), the relation between ω_0 and D can be expressed by

$$\frac{L_2 C_2^2 R_{\mathrm{L}}}{2}\omega_0^3 - \frac{L_1 C}{\beta}\omega_0^2 + \left(\frac{2L_2}{R_{\mathrm{L}}} - \frac{C_2 R_{\mathrm{L}}}{2}\right)\omega_0 + \frac{C}{C_1 \beta} + \frac{\gamma}{\beta} = 0. \tag{12}$$

This is a cubic equation with a given D, and thus has three roots. Eq. (12) can be solved by MATLAB, and it can be seen that two roots are a pair of complex conjugates and one root is real. Frequencies are real numbers, so the complex roots are ineffective. The effective real root ω_0 with respect to D can be defined as $\omega_0 = f(D)$ (Fig. 4). It can be seen that a pair of D and ω_0 will satisfy Eq. (2) for a certain k. Therefore, the power link using the component values of Table 2 will operate in the optimum state.

Substituting $f(D)$ into Eqs. (1), (7), and (8), R_{eL}, R'_{eL} and X_{eL}, X'_{eL} with respect to D are obtained, as shown in Figs. 5a and 5b, respectively. We can see that R'_{eL} and X'_{eL} are in direct proportion to k^2, and intersect with R_{eL} and X_{eL} at two points when k<0.28, at one point when k=0.28, and at no point when k>0.28. At those intersections, design Eq. (2) is satisfied and the inductive power link will operate in the optimum state.

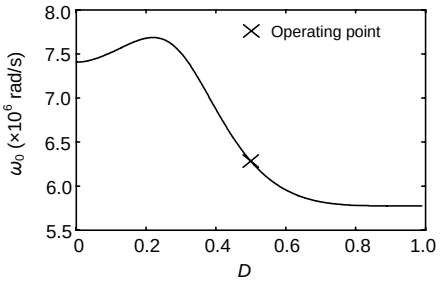

Fig. 4 Angular frequency with respect to duty cycle for the optimum state

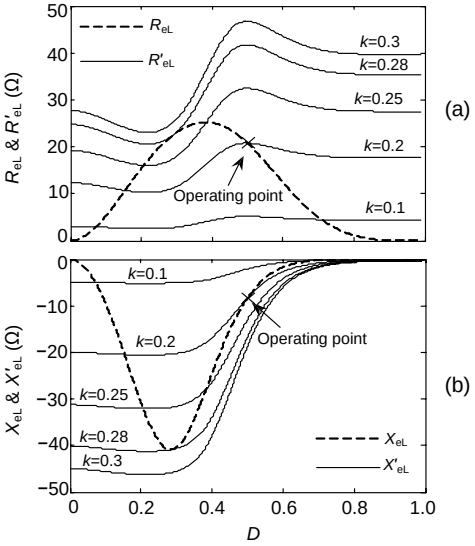

Fig. 5 Equivalent resistance and reflected resistance with respect to duty cycle

(a) Equivalent resistance and reflected resistance; (b) Equivalent reactance and reflected reactance

Combining Eqs. (1) and (7), k can be expressed as

$$k=\sqrt{\frac{\beta\left\{4R_{\mathrm{L}}^2+\left[\omega_0 L_2(4+\omega_0^2C_2^2R_{\mathrm{L}}^2)-\omega_0C_2R_{\mathrm{L}}^2\right]^2\right\}}{4\pi\omega_0^3L_1L_2R_{\mathrm{L}}C(4+\omega_0^2C_2^2R_{\mathrm{L}}^2)}}. \quad (13)$$

Substituting $f(D)$ into Eq. (13), k as a function of D and ω_0 is obtained. For a pair of D and ω_0, k is determined and in turn, for a certain k, there is a pair of D and ω_0 which will satisfy design Eq. (2). D and ω_0 with respect to k are shown in Figs. 6a and 6b, respectively. Both D and ω_0 need adjustment to maintain the optimum state of the power link when k varies.

Although the power link can be kept in the optimum state by adjusting D and ω_0 when k changes, R'_{eL} is charged. Thus P_{out} will be changed. To keep P_{out} constant, V_{DD} needs to be adjusted.

Combining Eqs. (7) and (9), V_{DD} can be expressed as

$$V_{\mathrm{DD}}=\sqrt{\frac{\alpha P_{\mathrm{in}}}{2\pi\omega_0C\sin\theta_{\mathrm{X}}}}. \quad (14)$$

Substituting $f(D)$ into Eq. (14), V_{DD} with respect to k is obtained. This relation is the ideal feedback control rule of V_{DD} to keep P_{out} constant when k varies (Fig. 6c). In a real circuit, power loss of each component exists and varies for different R_{eL} and D (Kessler and Kazimierczuk, 2004; Mury and Fusco, 2006). To keep P_{out} constant, V_{DD} needs additional adjustment when k varies.

Substituting $f(D)$ into Eq. (6), I_{o1m} with respect to k is obtained (Fig. 6d). I_{o1m} varies with k to keep P_{RF} constant due to the variation in R'_{eL}. From Eq. (4), I_{DD} with respect to k is derived. I_{DD} varies with k to keep P_{in} constant.

3.2 Feedback control

The power link will operate in the optimum state with constant output power if D, ω_0, and V_{DD} vary (Figs. 6a–6c). To detect the k variations, the phase difference θ_{PD} is employed as the feedback quantity. From Eqs. (5) and (13), θ_{PD} with respect to k can be determined (Fig. 6e). The variation range of k is set to $0.1\leq k\leq 0.25$, and the variation region of the feedback quantity is $2.17\leq\theta_{\mathrm{PD}}\leq 2.78$ (the bold line in Fig. 6e).

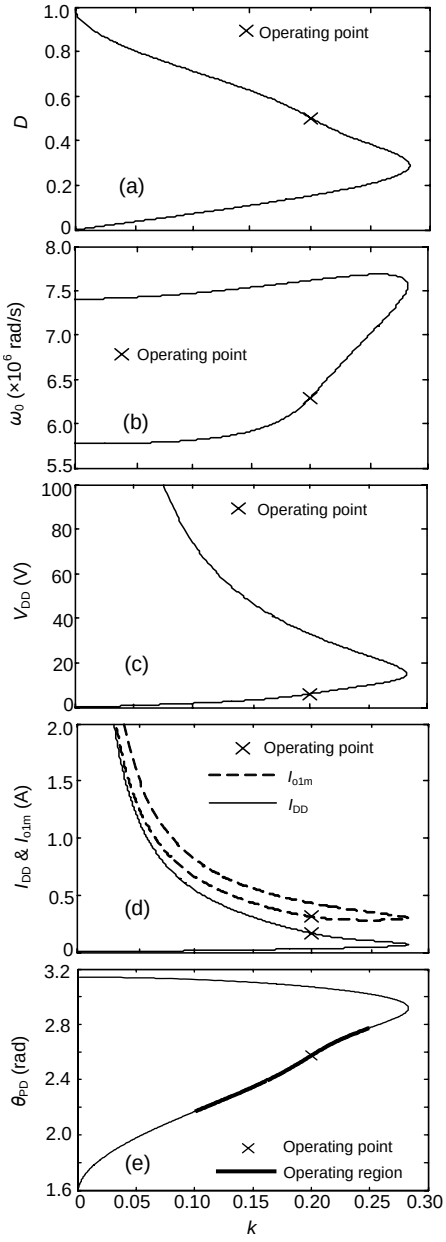

Fig. 6 Main parameters with respect to the coupling coefficient

(a) Duty cycle; (b) Angular frequency; (c) Supply voltage; (d) Input current and the amplitude of the output current; (e) Feedback quantity

From Eqs. (5) and (12), D and ω_0 can be expressed as functions of θ_{PD} (Figs. 7a and 7b, respectively). From Eqs. (5), (12), and (14), V_{DD} with respect to θ_{PD} is obtained (Fig. 7c).

To implement the control rules, θ_{PD} can be detected by a phase detector, and a microprocessor can be used to adjust D, ω_0, and V_{DD}.

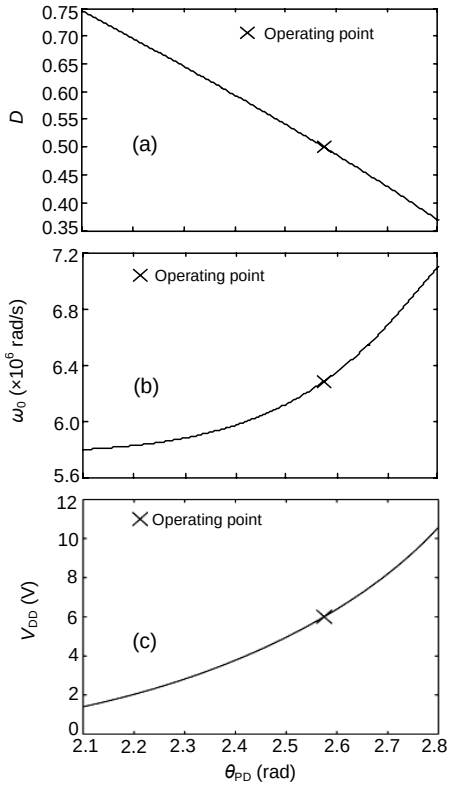

Fig. 7 Adjusted parameters with respect to feedback quantity
(a) Duty cycle; (b) Angular frequency; (c) Supply voltage

Table 1 Design parameters of the power link

Parameter	Value
Output power, P_{out}	1 W
Supply voltage, V_{DD}	6 V
Quality factor, Q	10
Duty ratio, D	0.5
Operating frequency, f	1 MHz
Coupling coefficient, k	0.2
Load resistance, R_L	1 kΩ

Table 2 Component values of the power link

Component	Value	ESR (Ω)
Choke coil, L_f	144.0 μH	0.18
Shunt capacitance, C	1.41 nF	0.21
Series inductance, L_1	33.0 μH	0.93
Series capacitance, C_1	907.3 pF	0.16
Resonance inductance, L_2	31.8 μH	0.86
Resonance capacitance, C_2	795.8 pF	0.14
Equivalent resistance, R_{eL}	20.8 Ω	–

ESR: equivalent series resistance

4 Experimental results

To experimentally validate the operating state and the output power of the inductive power link when the relative position between the transmitter coil and the receiver coil changes, an inductive power link was designed which satisfies the parameters given in Table 1. Based on the component determination equations shown in Section 2, the component values are shown in Table 2.

The MOSFET IRF 510 was employed as the switch. The driving signals were derived from a function generator. All capacitors were Silver Mica, and the inductive coils were made of Litz wire, which consists of 200 strands with a diameter of 0.1 mm. The primary and secondary coils were 19 and 18.75 turns respectively, with a diameter of 85 mm. The capacitors, the inductor, and their equivalent series resistances (ESR) were measured using an HP LF Impedance Analyzer 4192 A in the laboratory at the intended operating frequency of 1 MHz (Table 2). The coupling coefficients between the RF coil pair were calculated using the equation $U_2=kL_1L_2\omega_0 I_1$. I_1 is the current of the primary coil and U_2 is the induced voltage of the secondary coil. The primary coil was driven by a 1 MHz sine wave, which was derived by the function generator. The voltages of the primary and secondary coils were measured and then k could be calculated. It was found that the coupling coefficients between the coil pair were 0.1, 0.2, and 0.25 when their center distances were 69, 46, and 40 mm, respectively.

The primary circuit adopted the basic Class-E amplifier (Fig. 3) and the secondary circuit was simplified using the linear model (Fig. 2). The minimum and maximum values of k were set to 0.1 and 0.25, respectively. For different k's, the adjustments of D, frequency f ($=\omega_0/(2\pi)$), and V_{DD} are shown in Table 3.

P_{out} was calculated by $P_{out}=V_o^2/R_L$, where V_o is the effective value of v_o. P_{in} is determined by V_{DD} and I_{DD}. Each component of the power link has parasitic resistance, and power loss will exist. P_{out} may be smaller than that designated. To satisfy the require-

ment of constant output power of 1 W, V_{DD} needed to be adjusted. V_{DD} was adjusted to 2.6, 6.4, and 10.4 V when k was 0.1, 0.2, or 0.25, respectively. The adjustments of V_{DD} were slightly larger than the theoretical values of 1.8, 6, and 9.9 V.

The experimental switch voltages v_S and output voltages v_o of the secondary circuit are shown in Fig. 8. The waveforms of the power link with a k of 0.2 are shown in Fig. 8b. It can be seen that v_S returned to zero smoothly when the switch turned on. The slope of v_S will be zero at the instant the switch turns on, and thus the power link will operate in the optimum state; the amplitude of v_o was 31.6 V and P_{out} was 1 W. In Figs. 8a and 8c, the waveforms of the power link with and without adjustments are plotted on the left and right when k was 0.1 and 0.25, respectively. It can be seen that the power link with the adjustments to D, ω_0, and V_{DD} will operate in the optimum state with constant output power; without any adjustment, the power link will not maintain its optimum state and the output power will reduce. In the no-adjustment condition, the amplitudes of the output voltage were 16.5 V and 24.4 V, and the output powers were 272 mW and 595 mW when k was 0.1 and 0.25, respectively. These values are much smaller than those designated.

There are parasitic resistances in the components of the primary and secondary circuits. To analyze the efficiency of the circuits, the primary efficiency η_p is defined as the total efficiency of the primary circuit except the driving signal, and the secondary efficiency η_s is the total efficiency of the secondary circuit. With the ESR of each component, η_p, η_s, and the theoretical total efficiency η_c were calculated (Fig. 9) (Yang *et al*., 2009). The experimental total efficiency with adjustments η_{ac} and the experimental total efficiency without any adjustment η_{nc} are plotted in Fig. 9. It can be seen that η_{ac} closely matches η_c; without any adjustment, the efficiency would decrease significantly, especially for the small k condition.

The experimental input power, output power, and efficiency are shown in Table 3. η_{ac} was 67.6% when the coupling coefficient k was 0.1, which was much smaller than when k was 0.2 or 0.25. The reason is that the equivalent load resistance R_{eL} is only 4.6 Ω at k=0.1. This is so small that the parasitic resistance of each component will significantly affect the circuit. A large R_{eL} will decrease the effect of parasitic resistances and reduce the component power loss, thereby increasing efficiency.

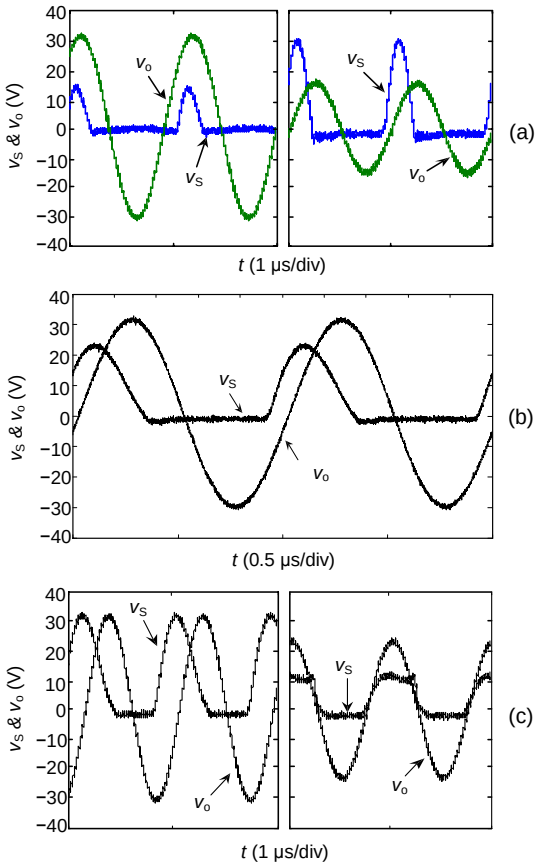

Fig. 8 Waveforms of switch voltage and output voltage
(a) k=0.1; (b) k=0.2; (c) k=0.25

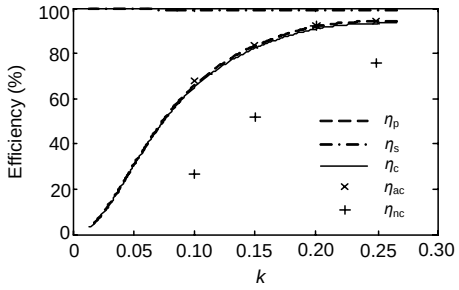

Fig. 9 Computed and measured efficiencies with respect to the coupling coefficient *k*
η_p: primary efficiency; η_s: secondary efficiency; η_c: theoretical total efficiency; η_{ac}: experimental total efficiency with adjustments; η_{nc}: experimental total efficiency without any adjustment

Table 3 Adjusted parameters, power, and efficiency

Parameter	Value		
	k=0.1	k=0.2	k=0.25
Equivalent resistance, R_{eL} (Ω)	4.6	20.8	25.2
Duty cycle, D	0.71	0.75	0.38
Frequency, f (MHz)	0.925	1.000	1.113
Supply voltage, V_{DD} (V)	2.6	6.4	10.4
Input power, P_{in} (W)	1.48	1.09	1.06
Output power, P_{out} (W)	1.00	1.00	1.00
Experimental total efficiency with adjustments, η_{ac} (%)	67.6	91.7	94.3

5 Conclusions

In this paper, a feedback analysis of an inductive power link driven by a Class-E amplifier with a variable coupling coefficient is presented. Analytical design equations are derived at any duty cycle using an impedance-analysis method. Feedback analyses are evolved from the design equations. In feedback control, both the duty cycle and frequency of the driving signal are adjusted to keep the power link tuning, and the supply voltage is controlled to keep the output power constant when the coupling coefficient is changed. The phase difference between the output current of the Class-E amplifier and the driving signal is used as a feedback quantity. The relations between the adjusted parameters and the coupling coefficient, and the feedback quantity are derived in a design example with a coupling coefficient of 0.2 and a duty cycle of 0.5. An experiment was conducted to validate the control functions. The results showed that the inductive power link operated in the optimum state with constant output voltage by adjustment of the duty cycle, the frequency of the driving signal, and the supply voltage when the coupling coefficients changed from 0.2 to 0.1 to 0.25.

References

Baker, M.W., Rahul, S., 2007. Feedback analysis and design of RF power links for low-power bionic systems. *IEEE Trans. Biomed. Circ. Syst.*, **1**(1):28-38. [doi:10.1109/TBCAS.2007.893180]

Donaldson, N.N., Perkins, T.A., 1983. Analysis of resonant coupled coils in the design of radio frequency transcutaneous links. *Med. Biol. Eng. Comput.*, **21**(5):612-627. [doi:10.1007/BF02442388]

Kazimierczuk, M.K., Czarkowski, D., 1995. Resonant Power Converters. Wiley, New York.

Kendir, G.A., Liu, W., Wang, G., Sivaprakasam, M., Bashirullash, R., Humayun, M.S., Weiland, J.D., 2005. An optimal design methodology for inductive power link with Class-E amplifier. *IEEE Trans. Circ. Syst.-I*, **52**(5):857-868. [doi:10.1109/TCSI.2005.846208]

Kessler, D.J., Kazimierczuk, M.K., 2004. Power losses and efficiency of Class-E power amplifier at any duty ratio. *IEEE Trans. Circ. Syst.-I*, **51**(9):1675-1689. [doi:10.1109/TCSI.2004.834505]

Ko, W.H., Liang, S.P., Fung, C.D.F., 1977. Design of radio-frequency powered coils for implant instruments. *Med. Biol. Eng.*, **15**(6):634-640. [doi:10.1007/BF02457921]

Lenaerts, B., Puers, R., 2007. An inductive power link for a wireless endoscope. *Biosens. & Bioelectron.*, **22**(7):1390-1395. [doi:10.1016/j.bios.2006.06.015]

Lenaerts, B., Puers, R., 2008. Automatic inductance compensation for Class-E driven flexible coils. *Sens. & Actuat. A*, **145-146**:154-160. [doi:10.1016/j.sna.2007.11.011]

Mury, T., Fusco, V.F., 2006. Analysis and synthesis of pHEMT class-E amplifiers with shunt inductor including ON-state active-device resistance effects. *IEEE Trans. Circ. Syst.-I*, **53**(7):1556-1564. [doi:10.1109/TCSI.2006.876416]

Raab, F.H., 1977. Idealized operation of the Class-E tuned power amplifier. *IEEE Trans. Circ. Syst.*, **24**(12):725-735. [doi:10.1109/TCS.1977.1084296]

Sarpeshkar, R., Salthouse, C., Sit, J.J., Baker, M.W., Zhak, S.M., Lu, T.K.T., Turicchia, L., Balster, S., 2005. An ultra-low-power programmable analog bionic ear processor. *IEEE Trans. Biomed. Eng.*, **52**(4):711-727. [doi:10.1109/TBME.2005.844043]

Sokal, N.O., Sokal, A.D., 1975. Class E: a new class of high-efficiency tuned single-ended switching power amplifiers. *IEEE J. Sol.-State Circ.*, **10**(3):168-176. [doi:10.1109/JSSC.1975.1050582]

Wang, G., Liu, W., Sivaprakasam, M., Kendir, G.A., 2005. Design and analysis of an adaptive transcutaneous power telemetry for biomedical implants. *IEEE Trans. Circ. Syst.-I*, **52**(10):2109-2117. [doi:10.1109/TCSI.2005.852923]

Yang, T.L., Zhao, C.Y., Zhang, J.Y., Chen, D.Y., 2009. Power Loss and Efficiency of Transcutaneous Energy Transmission System with Class-E Power Amplifier at Any Duty Ratio. Int. Symp. on Signals, Circuits and Systems, p.425-428. [doi:10.1109/ISSCS.2009.5206221]

Zan, P., Yan, G., Liu, H., Luo, N., Zhao, Y., 2007. Adaptive transcutaneous power delivery for an artificial anal sphincter system. *J. Med. Eng. Technol.*, **33**(2):136-141. [doi:10.1080/03091900801943205]